A Hybrid Optimization for Pattern Synthesis
of Large Antenna Arrays

Jiazhou Liu[1, 2], Zhiqin Zhao[1, *], Kai Yang[1], and Qing-Huo Liu[2]

Abstract—The pattern synthesis for large antenna arrays has drawn significant attention because of its wide applications. This paper introduces a hybrid approach for the fast pencil beam pattern synthesis of the large non-uniform linear or planar array, which can significantly reduce the computational cost, the number of antenna in the array, the minimum sidelobe level and the null control. The proposed method has an iterative scheme which is composed of the nonuniform Fourier transform (NUFFT) and the global optimization method to minimize the peak sidelobe level and control the null. The NUFFT is utilized to determine excitation magnitudes for a fixed positions non-uniform array. Alternatively, the global optimization is used to find the optimal positions which lead to the minimum peak sidelobe level (PSL). The lower excitations can be deleted due to yielding less performance on sidelobe level, which is called the array removal strategy. Compare with conventional methods, the simulations on synthetic models show that a minimum sidelobe level and null control can be obtained in processing sparse linear and concentric circular antenna arrays more efficiently.

1. INTRODUCTION

Antenna array has attracted growing attention in a wide range of applications, such as sonar, radar, and mobile communications. The conventional methods which avoid the grating lobe, such as the Dolph-Chebyshev [1] and the Taylor-Kaiser methods [2], are well known for synthesizing a narrow beam and low sidelobe in a uniformly spaced array. However, the antenna arrays obtained from these methods are densely spaced, and the array requires a large number of elements to radiate the desired pattern. Large array limits the usage of the applications, especially for the radar on aircrafts or satellites.

The synthesis of nonuniformly spaced antenna arrays has much more freedom to improve array performance. Several practical techniques have been developed to optimize the element positions and the excitations for pattern synthesis or to obtain a given pattern [3–5]. The problem addressed in this paper is to optimize the antenna element excitations and positions for synthesizing peak sidelobe level (PSLL) and controlling the null with minimum number of antennas, especially for large linear and planar arrays. There are several array pattern synthesis techniques, such as the analytical method [6], the synthesis techniques [7–9], the global optimization, the convex optimization and the hybrid methods for lowing peak sidelobe levels. The global optimization includes the particle swarm optimization (PSO) [10–12, 17], the simulated annealing (SA) [13, 14], and genetic algorithms (GA) [15, 16]. Although these methods have been successfully used in the design of antenna arrays, challenges still exist. For example, these methods easily fall into local optimization, the computation cost is huge and grow rapidly with the antenna array size. The PSO algorithm proposed in [17] is used to synthesis the linear array with a minimum sidelobe level and null control. Due to whole array uses identical excitation, the variances are positions only. Therefore, the PSLL obtained from the PSO algorithm is hard to be minimized.

Compared to the PSO algorithm, the pattern synthesis methods are proposed in a convex form [18–20] to optimize the excitations and positions. They can be solved with a good performance by SeDuMi and CVX. However, these optimization solvers are complicated and have a relatively high computational cost for very large arrays due to superposition samples. The effective hybrid approach in [21, 22] uses antenna selection for the optimal synthesis of pencil beams. The approach takes advantage of the convexity property of the problem with respect to excitation variables, and exploits a simulated annealing procedure by treating element locations variables are concerned. Although the PSLL and the number of elements are used to control in this approach, the null control is skipped. Therefore, they cannot obtain a fully optimized solution.

Recently, an iterative fast Fourier transform (FFT) method [23] was presented to synthesize the large arrays with uniform element spacing. Through this method, it is found that there is an inverse Fourier transform relationship between the array factor and the element excitations. Then, [24] proposed the low-sidelobe pattern synthesis method with nonuniform element spacing, which the idea comes from the NUFFT [25]. The nonuniform distributed elements are firstly converted into a virtual uniform array, then apply FFT to synthesis SLL. This method has a much better computational performance for large arrays due to the efficiency of FFT. However, the positions must be known and fixed through the procedure. Therefore, the PSLL is not fully optimal and the number of the antenna cost is very large.

Thanks to the ideas of [16, 21], and [22], we propose a new hybrid approach based on nonuniform Fourier transform (NUFFT) and the global optimization to optimize the sidelobe level suppression, the null control and antenna layout. This method firstly initializes the array with a nonuuniform layout. With these element positions, the excitations are optimized. Each element in the initial nonuniform array is interpolated by several virtual uniform arrays. Therefore, the sparse antenna arrays are replaced by several virtual uniform arrays. The FFT is applied to optimize the virtual element excitations in order to achieve the minimum sidelobe level of the array pattern. Thereafter, the real excitations are calculated within a smaller interpolation error. With solved excitations on antennas, the layout of the array will be re-optimized and the position of each element will be re-located. Re-locating the positions is a nonlinear optimization, so a global optimization method can be used. Here, we employ the simulated annealing (SA), which has been verified as a good global optimization method. Finally, the approach uses the NUFFT with respect to excitations as variables, and exploits a SA procedure with element locations as variables alternatively until the sidelobe level is minimized with a maximally sparse array. Here, the antenna removal strategy [16] is used to re-optimize the number of the array elements when the new element excitations are obtained. Elements that contribute less to the array performance are removed systematically. The proposed method iteratively re-calculates the array excitations and re-locates the antenna array until the PSLL is unchanged or the maximum iteration number is reached. Therefore, the sidelobe level is minimized and the null level is controlled by adjusting the element positions and the excitation coefficients. The simulations on synthetic models show that, for large arrays, our method has a smaller PSLL than the CVX and the global optimization methods.

The paper is organized as follows. The sidelobe minimization based on the NUFFT and the basic concept of SA is present in Section 2. In Section 3, a hybrid optimization by adjusting the element positions and the excitation coefficients is discussed. The simulation results are given in Section 4. The last section is the conclusion.

2. PATTERN SYNTHESIS WITH THE NUFFT AND GLOBAL OPTIMIZATION

2.1. The NUFFT for Calculating the Array Excitation

The Fast Fourier Transform (FFT) [23] is utilized to obtain the minimum peak sidelobe level by adjusting the excitations in a uniform array. However, the antenna positions are usually preferred to achieve a sparse array. Thus, the traditional FFT cannot be applied. Fortunately, the NUFFT can handle this challenge very well. First, for a linear antenna array with M identical elements, the element positions can be defined as $\mathbf{d} = [d_1, d_2, \ldots, d_M]^T$, where d_i represents the position of the i-th element. The array factor can be written as

$$AF(u) = \sum_{i=1}^{M} w_i e^{jkd_i u} \tag{1}$$

where $j = \sqrt{-1}$, $k = 2\pi/\lambda$ is the wave number, λ the wavelength, $\mathbf{w} = [w_1, w_2, \ldots, w_M]^T$ the element excitations, and w_i the excitation located in i-th element. $u = \cos\phi$ is $[-1, 1]$, and ϕ is the angle between the direction of observation and the linear array.

To fix the nonuniform element positions, a optimization based on NUFFT with respect to the element excitations is employed to synthesis the nonuniform excitations. Here, the i-th element in the array is converted into the superposition of a virtual equally spaced array. Then, the nonuniform array is represented by a large uniform array. The interpolation function for each element factor can be written as

$$e^{j2\pi d_i u/\lambda} = \sum_{k=-q/2}^{q/2} x_k(d_i) e^{j2\pi t([rc_n]+k)/L} \tag{2}$$

where the left side of (2) is the i-th element factor, and the right side of (2) is the superposition of virtual equally spaced elements factor. $[rc_n]$ denotes the nearest integer of rc_n. q is an even positive integer representing the number of the virtual equally spaced element arrays. $x_k(d_i)$ is the virtual excitations and r the real integer oversampling factor which is larger than 1. $c_n = 2d_n/\lambda$ and $[rc_n] + k$ are the new virtual array positions. $t = uN/2$, which is the number of the uniform sampling points in $u \in [-1, 1]$. $L = rN$, $N = \lfloor c_n - c_1 \rfloor + p$. Here, q, p, and r determine the interpolation accuracy and the computational cost. How to choose q, p, and r is discussed in [24].

(2) can be present in a matrix and vector forms

$$\mathbf{A}\mathbf{x}(d_i) = \mathbf{v}(d_i) \tag{3}$$

where

$$\mathbf{x}(d_i) = [x_{-q/2}(d_i), x_{-q/2+1}(d_i), \ldots, x_{q/2}(d_i)]^T \tag{4}$$

$$\mathbf{A} = \begin{bmatrix} e^{j2\pi u(-N/2)([rc_n-q/2])/L} & e^{j2\pi u(-N/2)([rc_n-q/2+1])/L} & \cdots & e^{j2\pi u(-N/2)([rc_n+q/2])/L} \\ e^{j2\pi u(-N/2+1)([rc_n-q/2])/L} & e^{j2\pi u(-N/2+1)([rc_n-q/2+1])/L} & \cdots & e^{j2\pi u(-N/2+1)([rc_n+q/2])/L} \\ \vdots & \vdots & \ddots & \vdots \\ e^{j2\pi u(N/2)([rc_n-q/2])/L} & e^{j2\pi u(N/2)([rc_n-q/2+1])/L} & \cdots & e^{j2\pi u(N/2)([rc_n+q/2])/L} \end{bmatrix} \tag{5}$$

$$\mathbf{v}(d_i) = \left[e^{j2\pi d_i u(-N/2)/\lambda}, \, e^{j2\pi d_i u(-N/2+1)/\lambda}, \, \ldots, \, 1, \, \ldots, \, e^{j2\pi d_i u(N/2)/\lambda} \right]^T \tag{6}$$

Insert (2) into (1), (1) can be rewritten as

$$AF(u) = \sum_{i=1}^{M} w_i \sum_{k=-q/2}^{q/2} x_k(d_i) e^{j2\pi([rc_n]+k)t/L} = \sum_{l=1}^{L} \beta_l e^{j2\pi lt/L} \tag{7}$$

where $l = [rc_n] + k$, $\boldsymbol{\beta} = [\beta_1, \beta_2, \ldots, \beta_L]^T = \mathbf{T}\mathbf{w}$ contains the previous and new elements excitations, $\mathbf{T} \in C^{L \times M}$. The element at l-th row and nth column of the matrix $\mathbf{T}$ is given as

$$\mathbf{T}_{l,n} = \begin{cases} x_k(d_i), & l = [rc_n] + k, \, k = -q/2, \ldots, q/2 \\ 0, & \text{else} \end{cases} \tag{8}$$

Due to the fact that the matrix $\mathbf{T}$ is fixed during the procedure [24], it can be calculated once only. The matrix $\boldsymbol{\beta}$ is the excitations of the oversampling virtual uniform array. The matrix $\mathbf{w}$ is the excitations of the real nonuniform array, which is obtained by the least square, $\mathbf{w} = \mathbf{T}^\dagger \boldsymbol{\beta}$, where the superscript † stands for the Moore-Penrose pseudoinverse.

(7) can be rewritten in a matrix and vector form as well

$$\mathbf{AF} = \mathbf{A}\boldsymbol{\beta} \tag{9}$$

where $\mathbf{AF}$ is the matrix form of $AF(u)$. The matrix $\boldsymbol{\beta}$ is obtained by least square, $\boldsymbol{\beta} = \mathbf{A}^\dagger \mathbf{AF}$, where the superscript † stands for the Moore-Penrose pseudoinverse.

After the interpolation is finished, the nonuniform arrays are converted into virtual uniform arrays. The excitations β_l for the virtual array are optimized by the iterative FFT method. The details of the iterative FFT are referred in [23]. The updating schema to solve element excitations in the proposed method is shown as follows:

a) The oversampled virtual uniform arrays are obtained by (2); define the mainlobe region, the silelobe region, the null regions, the desired PSLL and null value; define the q, p, and r, respectively.

b) Initialize the excitation randomly, calculate $\mathbf{x}(d_i)$ by (3) with the least square method and obtain matrix $\mathbf{T}$ by (8), then obtain the initial $\boldsymbol{\beta}$ by (9).

c) Apply a K points IFFT to $\boldsymbol{\beta}$, the array pattern is obtained.

d) Find all values in the sidelobe region and null region, and adjust the sidelobes and nulls whose values are greater than the desired PSLL and null. If all the values of the sidelobes are less than the desire PSLL, the desire PSLL is decreased by 0.5 dB.

e) Utilize the FFT to adjust the pattern, and then obtain the new $\boldsymbol{\beta}$.

f) Repeat the steps c)–e) until all the sidelobe values are smaller than the desired PSLL or the number of the maximum iteration is reached.

In addition, this method can be extended to two-dimension, in which, (2) can be rewritten as

$$e^{j2\pi(d_x u + d_y v)/\lambda} = \sum_{k_x=-q/2}^{q/2} \sum_{k_y=-q/2}^{q/2} a_{k_x}(d_x) a_{k_y}(d_y) \times e^{j2\pi(([rc_x]+k_x)t_x/L_x + ([rc_y]+k_y)t_y/L_y)} \tag{10}$$

where (d_x, d_y) is the element position. $u = \sin\theta\cos\phi$, $v = \sin\theta\sin\phi$, $c_x = 2d_x/\lambda$, $c_y = 2d_y/\lambda$, $t_x = uM_x/2$, $t_y = uM_y/2$, $L_x = rM_x$, and $L_y = rM_y$. (θ, ϕ) is the impinged angle. The 2D NUFFT is similar to the 1D NUFFT. The virtual excitations in x and y-axis are obtained by the least square method. Then, the transformation matrix $\mathbf{T}$ is constructed. The procedure of the 1D NUFFT can be similarly utilized in 2D.

2.2. The Simulated Annealing Method

The SA is a general probabilistic algorithm used in a fixed period of time to find an optimal solution in a large searching space, which is introduced by S. Kirkpatrick et al. The idea is similar to the metal annealing approximation principle. To apply the theory of thermodynamics to statistics, every point within the searching space can be treated as the air molecular. Then, an energy function with respect to molecular will be minimized. The energy function is the fitness function with respect to positions. The main idea is to find the optimization results of the element positions within fixed element weights in order to minimize the PSLL and control the null. The fitness function [17] is defined as

$$\text{Fitness}(\mathbf{d}_n) = \sum_i \frac{1}{\Delta u_i} \int_{u_{li}}^{u_{ui}} |AF(u)|^2 \, du + \sum_k |AF(u_k)|^2 \tag{11}$$

where $[u_{li}, u_{ui}]$ are the spatial regions in which the SLL is restricted. $\Delta u_i = u_{ui} - u_{li}$ and u_k are the direction of the sidelobe and nulls (if necessary). $\mathbf{d}_n$ is the vector of position variables, which can be 1D or 2D. The first term on the right-hand side of (11) is used to evaluate the sidelobe level and the second term is used to evaluate the null level.

The maximum temperature, iteration number, positions variables are initialized. The sidelobe and null ranges are given in NUFFT process. The method has an annealing schedule which contains the cooling procedure, the cooling rate, and the stop threshold. After reaching the maximum iteration number, the temperature is decreased with the cooling rate. For each iteration (n is the iterative number), if the new position $\mathbf{d}_n$ cause the fitness function decrease, it is accepted ($\mathbf{d}_{n+1} = \mathbf{d}_n$). Otherwise, if the new positions $\mathbf{d}_n$ cause the value of the fitness function to increase, it is acceptable only there is a probability criterion on the system temperature in accordance with Metropolis manner. The higher temperature introduces bigger difference and cause a higher probability as

$$P(\mathbf{d}_{n+1} = \mathbf{d}_n) = \begin{cases} e^{-\Delta f/T}, & \text{if } \Delta f \leq 0 \\ 1, & \text{if } \Delta f > 0 \end{cases} \tag{12}$$

where $P(x)$ is a probability coherent with current temperature. $\Delta f = f' - f$ is the difference value between the fitness f in n iteration and fitness f' in $n+1$ iteration.

To update the positions $\mathbf{d}_n$ is important for the global optimization due to non-linear problem. The position update procedure of PSO is utilized to generate the new position in an iteration of the algorithm [18]. To achieve this, the velocity is updated as follows

$$\mathbf{v}_{n+1} = w * \mathbf{v}_n + (C_1 * \text{rand1}()) * (\mathbf{P}_i^n - \mathbf{d}_n) + (C_2 * \text{rand2}()) * (\mathbf{P}_g^n - \mathbf{d}_n) \tag{13}$$

where n and $n+1$ represent the iteration index. $\mathbf{P}_i^n$ and $\mathbf{P}_g^n$ are the best position and the global best position in the n-th iteration, respectively. C_1 and C_2 are the acceleration coefficients. w is the inertia weight given by [17]. A large inertia weight is preferred to explore the whole search space. However, a smaller inertia weight is required to exploit around the local area. Therefore, the position is updated in iteration as

$$\mathbf{d}_{n+1} = \mathbf{d}_n + \mathbf{v}_n \tag{14}$$

The SA procedure stops until the temperature is lower down to the minimum. The re-located positions are obtained after the SA procedure finish.

3. A HYBRID APPROACH WITH THE ANTENNA REMOVAL STRATEGY

With the aim to minimize the sidelobe level and the null control with fewer elements, a hybrid approach is used to adjust the excitations and positions of the antenna array. The minimization of the number of array is then achieved by iteratively removing the elements that contribute the least to the array factor. The antenna removal strategy [16] is utilized to achieve this goal.

Obviously, to remove elements in antenna array distort the array pattern inevitably, such as the PSLL increased and the mainlobe changed. In order to calculate this effect, the removal factor, δ_i, is defined as the PSLL performance when removing one of elements.

$$\delta_i = \frac{|\text{PSL}_{\text{org}}| - |\text{PSL}_i|}{|\text{PSL}_{\text{org}}|} \tag{15}$$

where PSL_{org} is the original PSL and PSL_i is the PSL which removes the i-th element.

We can use an example to demonstrate the performance. Considering a 170-elements nonlinear array with a sidelobe range as $0.0048 \leq |\cos(\phi)| \leq 1$, the relationship between the removal factor δ_i and w_i is shown in Figure 1. The figure implies that elements with smaller excitation are likely to contribute less to the PSLL. Hence, the sensors with excitations smaller than the threshold value w_t can be removed from the array with a smallest effect. The detail of the removal strategy is introduced in [16]. Based on our observation, the threshold w_t is better in the range of $[0.25w_{\text{max}}, 0.4w_{\text{max}}]$.

The overall procedure is summarized in the flow chart of Figure 2, where i and j are represented to the iteration number of the whole procedure and the global optimization, respectively. The desired PSLL is set to determine whether the removal array strategy is implemented. In particular, the initial
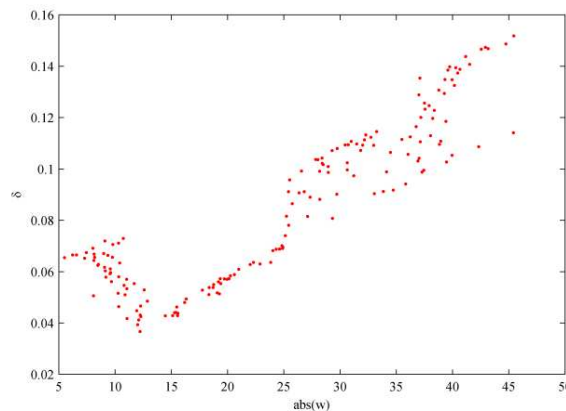

Figure 1. The relationship between the PSL and the removal weight.
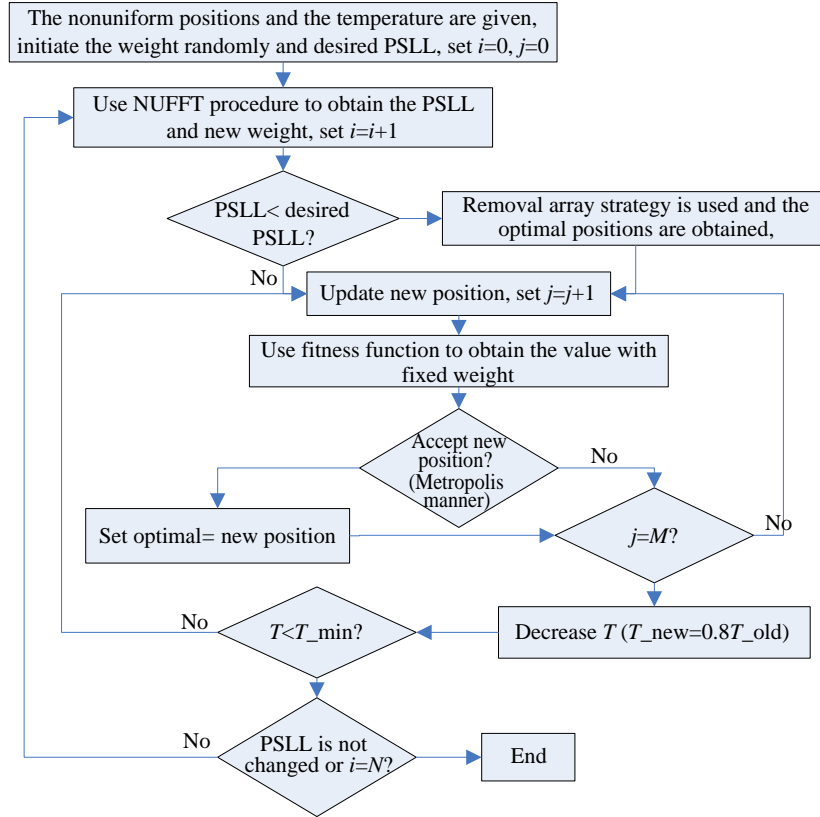
Figure 2. Flow chart of the proposed hybrid approach.

nonuniform positions are provided by the MPM [3] in the first step and the weight is initiated randomly. Then, this approach is alternately used the NUFFT and the SA. In the NUFFT step, the nonuniform positions are fixed to use the FFT with respect to the excitations. After several iterations, the PSLL and the new weights are obtained. If the obtained PSLL is smaller than the desired PSLL, the removal array strategy is used to delete the elements which have less contribution to the PSLL. Thereafter, the SA step is carried out. The fitness value is calculated from finding the minimum value with fixed weights. Compared to the original value, the Metropolis manner is used for accepting the new optimal values with new positions. After the new positions are obtained, the number of the updated position is determined. If it does not reach the minimum temperature, go back to the position updating process with a decreased temperature. Then reaching the minimum temperature, the SA step is done, then go back to the NUFFT process if the PSLL is not changed or the i doesn't reach the maximum. Finally, the PSLL, the element positions and the excitations are obtained alternatively.

4. SIMULATION

In order to assess the efficiency of the proposed method, several simulations were performed for the pattern synthesis. The simulations employ large nonuniform linear arrays and concentric circular arrays with low SLL and null control. In all cases, the mainlobe is unchanged.

4.1. Minimize the PSLL for Large Linear Array

This example uses a 678-element sparse linear array, whose element positions are given by MPM. The array aperture is initialized to 249.46λ, the half power beam width is $0.4°$ and the desired PSLL is -34 dB, which is the threshold to determine whether the removal array strategy will be performed. In the NUFFT process, $r = 1.5$, $q = 8$ and $p = 4$ are chosen. The iteration number in NUFFT is

Table 1. The simulation results in the CVX, the PSO, and the Proposed method with different initial elements.

Elements	CVX		PSO		Proposed method	
	PSLL (dB)	Element	PSLL (dB)	Element	PSLL (dB)	Element
403	−28.82	263	−20.52	282	−27.87	263
524	−33.04	384	−23.76	375	−32.23	384
628	−34.17	450	−25.54	432	−34.42	450
737	Failed	521	−31.57	515	−44.78	521
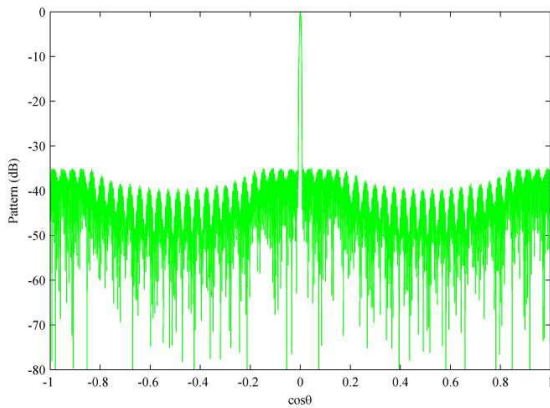
Figure 3. The pattern synthesis with 473 elements, the PSLL is −35.12 dB.
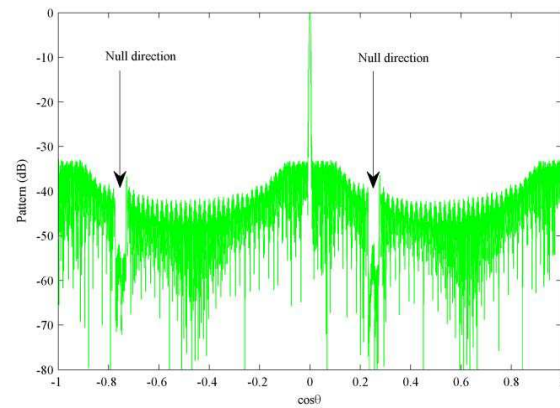

Figure 4. The array pattern with 247 elements and all the null regions are smaller than −52 dB.

3000. The initial temperature is 30°, and the minimum temperature is 1°. The iteration number of position updating is 200. The simulation result shows that the PSLL of the pattern is −35.12 dB with 473 elements, as shown in Figure 3. The proposed method saves 30% antenna. As a comparison, the CVX is carried out on this problem as well, and the optimized PSLL is equal to −34.95 dB. In addition, the optimized PSLL from the stochastic algorithm (here, we use PSO) is −26.43 dB with 463 elements. The excitation amplitude dynamic range ratio ($|w_{max}|/|w_{min}|$, DRR) is found to be 3.8427. Table 1 shows the PSLL and the reduced array number in CVX, PSO, and the proposed method with different initial elements. The PSLL of the CVX is better than the proposed method in smaller array due to the initial element positions of the CVX are given by the proposed method, only the excitations are required to be optimized. If the initial positions are not provided appropriately, the CVX maybe time consuming. Table 1 shows that the CVX is failed when the element number is increased to a relative large number. The CVX is failed when the element number is 737. This case validates that the proposed method has a better performance than others methods in PSLL.

4.2. PSLL Minimum and Null Control for Large Linear Array

In this case, the null control is added into design requirement for a sparse linear array. The sparse element positions are given by the matrix pencil method also. The pattern is the Chebyshev without null region. A 353-elements array is initialized from the matrix pencil method and the array aperture is 349.46λ. The desired pattern is to minimize the PSLL and control the null with a prescribed mainlobe area as [−0.036, 0.036]. In addition, two regions, [−76.7°, −74.4°] and [14.1°, 15.9°], are restricted to be smaller than −52 dB, which are represented to the null regions. The optimization objective is to set them lower than −52 dB in the null regions; in the all the other regions of the sidelobe, the optimization objective is to minimize the peak sidelobe level. The parameters r, q, and p are chosen as 2, 8, and 8,

respectively. Figure 4 shows the PSLL is equal to $-32.23\,\mathrm{dB}$ and the null regions are smaller than $-52\,\mathrm{dB}$ with the 247 elements. Obviously, the number of array elements is reduced more than 30% through the proposed method. The DRR is found to be 3.9228. As a comparison, the PSLL of the CVX is $-32.18\,\mathrm{dB}$ with the positions given by the proposed method. In addition, the PSO decreases the PSLL to $-19.83\,\mathrm{dB}$ with 251-element. Therefore, we know that the proposed method has a better performance on the PSLL and null control in large linear array.

4.3. Minimize the PSLL for a Concentric Circular Array

In the third example, a 2D concentric circular array is utilized to demonstrate that the proposed method can handle 2D array with high efficient as well. A concentric circular array is a planar array with elements lying on a circle. Several arrays with different radii can share a common center. Here, 20 rings and a single element at the center are used. The radius of the n-th array is $r_n = 0.6n\lambda$. Each ring has $\lceil 2\pi n \rceil$ elements equally spaced in a circle. The total elements number is 1310. The iteration number in the NUFFT is 5000. The mainlobe region is restricted to $\{(u,v)|\sqrt{u^2+v^2} \leq 0.074\}$. The parameters r, q, and p are chosen as 2, 16, and 12, respectively. The desired PSLL is $-35\,\mathrm{dB}$. Figure 5 shows the 3D array pattern with 718 elements and $-37.05\,\mathrm{dB}$ PSLL. Only 55% antenna array is used in this case. The v-cut pattern of the array is shown in Figure 6. Due to the large number of elements, the CVX cannot handle this problem anymore. As a comparison, the PSLLs in the PSO and the IWO-IFT [26] are $-26.92\,\mathrm{dB}$ with 730 and $-27.13\,\mathrm{dB}$ with 694 elements, respectively. The PSLLs are much worse than the array comes from the proposed method.
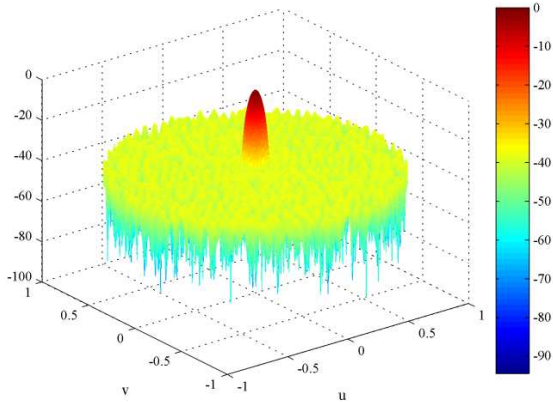

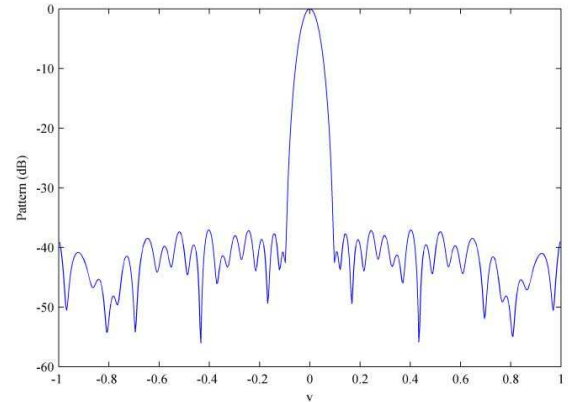**Figure 5.** The 3D pattern of the concentric circular array with 718 elements.

Figure 6. v-cut plot of the array pattern shown in Figure 5.

4.4. PSLL Minimum and Null Control for a Concentric Circular Array

The fourth case includes the PSLL and the null control optimization for a concentric circular array with same model in Example 3. The parameters r, q, and p are given as 1.5, 16, and 12. The number of virtual uniform element is 20960. The mainlobe region and the null region are restricted to $\{(u,v)|\sqrt{u^2+v^2} \leq 0.086\}$ and $\{(u,v)|-0.06 \leq u \leq -0.03, 0.67 \leq v \leq 0.78\}$, respectively. The iteration number in NUFFT is 5000. The null region is prohibited to be smaller than $-54\,\mathrm{dB}$ and the initial desired PSLL is $-33\,\mathrm{dB}$. Figure 7 shows the pesudocontour plot of the 3D pattern. The square in the figure is the null region. The v-cut pattern is in Figure 8. The proposed method obtains a 780-elements array, which saves 40% antenna array. The position of array elements is shown in Figure 9. The PSLL from the propose method is $-36.44\,\mathrm{dB}$. On the contrary, the CVX cannot be applied on this case because of the large array size is too large. The result from the IWO-IFT [26] has a PSLL of $-25.61\,\mathrm{dB}$ with 772 elements. The simulation shows the proposed method has a better performance on PSLL, and the null control in concentric circular array.
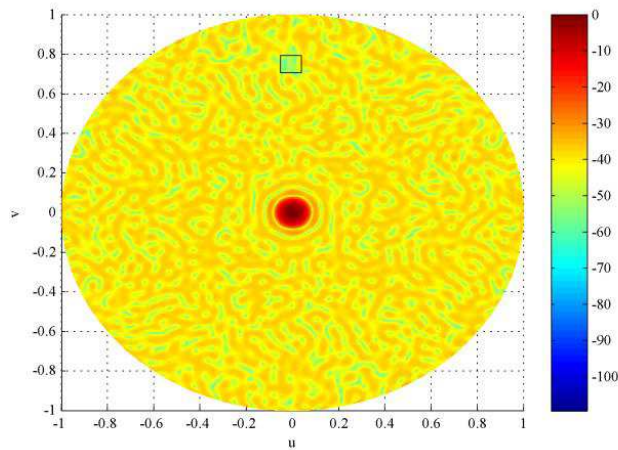
Figure 7. Pesudocontour plot of the concentric circular array with a null region, which is restricted to be smaller than -54 dB.
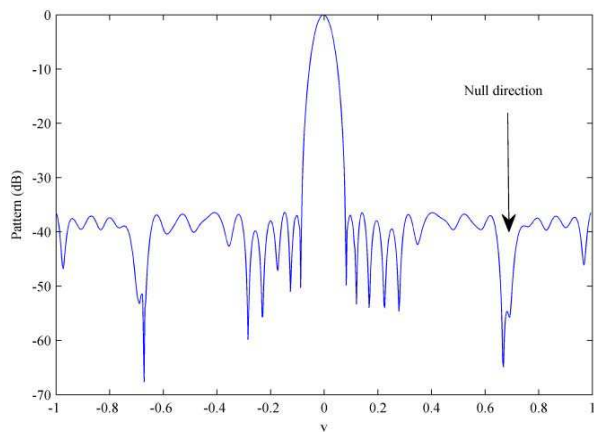

Figure 8. v-cut plot of the array pattern shown in Figure 7.
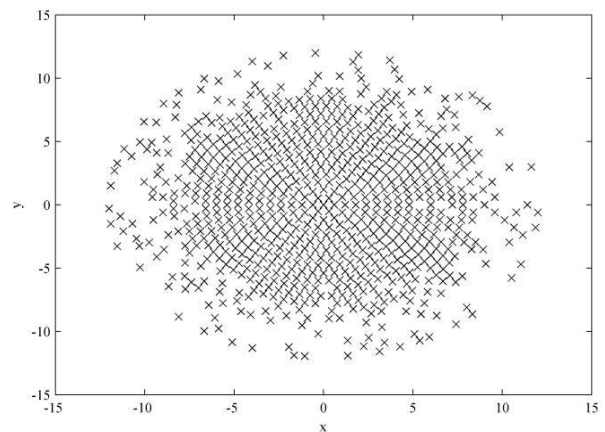

Figure 9. The location of 780-elements in the circular array.

5. CONCLUSIONS

A hybrid optimization approach based on the NUFFT and global optimization has been proposed for large nonuniform array pattern synthesis. The nonuniform arrays are interpolated by the several virtual uniform arrays. Then the FFT is used to minimize the peak sidelobe and control the null. Antenna removal strategy is applied after the new excitations are obtained. Then, to fix the new excitations, simulated annealing method is used to solve the optimal elements positions. The NUFFT and SA are combined to implement the pattern synthesis alternatively. The simulations illustrate that the proposed method is more efficient than the CVX and PSO for large arrays. Meanwhile, the PSLL and the null have a better control in the proposed method.

REFERENCES

1. Elliot, R. S., *Antenna Theory and Design,* Prentice-Hall, Englewood Cliffs, NJ, 1981.
2. Constantine, C. A. and A. Balanis, *Antenna Theory,* Wiley, New York, 1997.
3. Liu, Y. H., Z. P. Nie, and Q. H. Liu, "Reducing the number of elements in a linear antenna array by the matrix pencil method," *IEEE Trans. Antennas Propagat.*, Vol. 56, No. 9, 2955–2962, 2008.
4. Liu, Y. H., Z. P. Nie, and Q. H. Liu, "A new method for the synthesis of non-uniform linear arrays with shaped power patterns," *Progress In Electromagnetics Research*, Vol. 107, 349–363, 2010.
5. Oliveri, G. and A. Massa, "Bayesian compressive sampling for pattern synthesis with maximally sparse non-uniform linear arrays," *IEEE Trans. Antennas Propagat.*, Vol. 59, No. 2, 467–481, 2011.
6. Kumar, B. P. and G. R. Branner, "Generalized analytical technique for the synthesis of unequally spaced arrays with linear, planar, cylindrical or spherical geometry," *IEEE Trans. Antennas Propagat.*, Vol. 53, No. 2, 621–633, Feb. 2005.
7. Monorchio, A. and S. Genovesi, "An efficient interpolation scheme for the synthesis of linear arrays based on Schelkunoff polynomial method," *IEEE Trans. Antennas Wireless Propagat. Lett.*, Vol. 6, 484–487, 2007.
8. Recioui, A. and H. Bentarzi, "Null steering of dolph-chebychev arrays using taguchi method," *WSEAS Trans. Communications*, Vol. 9, 720–729, 2010.
9. Jarske, P., T. Sramaki, S. K. Mitra, and Y. Neuvo, "On the properties and design of nonuniformly spaced linear arrays," *IEEE Trans. Acoust., Speech, Signal Processing*, Vol. 36, 372–380, Mar. 1988.
10. Bevelacqua, P. J. and C. A. Balanis, "Minimum sidelobe levels for linear arrays," *IEEE Trans. Antenna Propagat.*, Vol. 55, No. 12, 2210–2217, Dec. 2007.
11. Nai, S. E., W. Ser, Z. L. Yu, and S. Rahardia, "Beampattern synthesis with linear matrix inequalities using minimum array sensors," *Progress In Electromagnetics Research M*, Vol. 9, 165–176, 2009.
12. Recioui, A., "Sidelobe level reduction in linear array pattern synthesis using particle swarm optimization," *Jour. of Optimization Theory and Applic.*, Vol. 153, 497–512, 2012.
13. Trucco, A., "Thinning and weighting of large planar arrays by simulated annealing," *IEEE Trans. Ultrason., Ferroelect., Freq. Control*, Vol. 46, No. 2, 347–355, Mar. 1999.
14. Trucco, A., E. Omodei, and P. Repetto, "Synthesis of sparse planar arrays," *Electron. Lett.*, Vol. 33, No. 22, 1834–1835, Oct. 1997.
15. Yan, K. K. and Y. Lu, "Sidelobe reduction in array-pattern synthesis using genetic algorithm," *IEEE Trans. Antennas Propagat.*, Vol. 45, No. 7, 1117–1122, Jul. 1997.
16. Cen, L., W. Ser, Z. L. Yu, S. Rahardja, and W. Cen, "Linear sparse array synthesis with minimum number of sensors," *IEEE Trans. Antennas Propagat.*, Vol. 58, No. 3, 720–726, Mar. 2010.
17. Khodier, M. M. and C. G. Christodoulou, "Linear array geometry synthesis with minimum sidelobe level and null control using particle swarm optimization," *IEEE Trans. Antennas Propagat.*, Vol. 53, No. 8, 2674–2679, Aug. 2005.
18. Yan, S. F. and J. M. Hovem, "Array pattern synthesis with robustness against manifold vectors uncertainty," *IEEE J. Ocean. Eng.*, Vol. 33, No. 4, 405–413, Oct. 2008.
19. Hoang, H. G., H. D. Tuan, and B.-N. Vo, "Low-dimensional SDP formulation for large antenna array synthesis," *IEEE Trans. Antennas Propagat.*, Vol. 55, No. 6, 1716–1725, Jun. 2007.
20. Nai, S. E., W. Ser, Z. L. Yu, and H. W. Chen, "Beampattern synthesis for linear and planar arrays with antenna selection by convex optimization," *IEEE Trans. Antennas Propagat.*, Vol. 58, No. 12, 3923–3930, Dec. 2010.
21. Isernia, T., F. J. A. Pena, O. M. Bucci, M. D'Urso, J. F. Gomez, and J. A. Rodriguez, "A hybrid approach for the optimal synthesis of pencil beams through array antennas," *IEEE Trans. Antennas Propagat.*, Vol. 52, No. 11, 2912–2918, Nov. 2004.
22. D'Urso, M. and T. Isernia, "Solving some array synthesis problems by mean of an effective hybrid approach," *IEEE Trans. Antennas Propagat.*, Vol. 55, No. 3, 750–759, Mar. 2007.

23. Keizer, W. P. M. N., "Fast low-sidelobe synthesis for large palnar array antennas utilizing successive fast Fourier transforms of the array factor," *IEEE Trans. Antennas Propagat.*, Vol. 55, No. 3, 715–722, Mar. 2007.

24. Yang, K., Z. Q. Zhao, and Q. H. Liu, "Fast pencil beam pattern synthesis of large unequally spaced antenna arrays," *IEEE Trans. Antennas Propagat.*, Vol. 61, No. 2, 627–634, Feb. 2013.

25. Liu, Q. H. and N. Nguyen, "An accurate algorithm for nonuniform fast Fourier transform (NUFFT's)," *IEEE Microw. Guided Wave Lett.*, Vol. 8, No. 1, 18–20, Jan. 1998.

26. Wang, X. K., Y. C. Jiao, Y. Liu, and Y. Y. Tan, "Synthesis of large planar thinned arrays using IWO-IFT algorithm," *Progress In Electromagnetics Research*, Vol. 136, 29–42, 2013.